Sea ice production and export from coastal polynyas in the Weddell and Ross Seas

Robert Drucker,[1] Seelye Martin,[1] and Ronald Kwok[2]

Received 24 June 2011; revised 2 August 2011; accepted 4 August 2011; published 8 September 2011.

[1] For 1992–2008, we use data from the Special Sensor Microwave/Imager (SSM/I) and the Advanced Microwave Scanning Radiometer-EOS (AMSR-E) to examine differences in ice production and export in the Weddell and Ross Seas. We find that the Ross production is three times that in the Weddell; the Ross export, twice that in the Weddell. In the Ross, the ice production has a statistically significant positive trend of about 21 km^3 y^{-1} and approximately equals the export, while in the Weddell, the production trend is statistically flat and provides only about 60% of the export. For each sea, comparison of the ice production with the total winter sea ice volume shows that the Weddell polynyas produce 5–10% of the total; the Ross polynyas, 20–50%. The explanation for these differences is that in the Ross, the low-pressure system is better situated for generation of large polynyas than in the Weddell. **Citation:** Drucker, R., S. Martin, and R. Kwok (2011), Sea ice production and export from coastal polynyas in the Weddell and Ross Seas, *Geophys. Res. Lett.*, *38*, L17502, doi:10.1029/2011GL048668.

1. Introduction

[2] For the Ross and Weddell Seas, this study compares the ice production in their coastal polynyas and the ice export across flux gates that lie over the 1,000-m depth contours. Polynyas are large, persistent regions of open water and thin ice that form adjacent to a lee shore within the pack ice. When winter winds advect the pack ice away from the coast, seawater at near freezing temperatures is exposed to a large negative heat flux, yielding rapid formation of new ice and brine rejection. As *Jacobs* [2004] describes, the polynyas and ice export of these two seas contribute to the formation of dense shelf water and the Antarctic bottom water. The Weddell has the largest winter Antarctic sea ice cover at 4.75×10^6 km^2, and the Ross has the second largest at 3.5×10^6 km^2 (National Snow and Ice Data Center (NSIDC) website, http://nsidc.org/data/smmr_ssmi_ancillary/regions). In both seas, polynya ice production and ice drift are driven by a low-pressure system located to the east. Because of the importance of these seas to shelf and deep-water production, and the similarity of their atmospheric forcing, we investigate the variability in their polynya ice production and ice export.

[3] In previous work in the Ross Sea and for 1992–2002, *Martin et al.* [2007] use the 25-km resolution SSM/I 37-GHz data to determine the distribution of thin ice thickness, and find that the mean annual polynya ice production is about 500 km^3 y^{-1}. *Martin et al.* [2007] and *Comiso et al.* [2011] also determine the net ice export from satellite feature tracking, and find that the export is in approximate balance with the production. For the Weddell, *Comiso and Gordon* [1998] show that polynyas occur along both the Ronne Ice Shelf and the east coast, and *Markus et al.* [1998] finds that of these polynyas, the Ronne is the largest producer.

2. Wind Patterns and Ice Motion

[4] For 2003–2008, days 90–300, Figures 1a and 1b show for the two seas, the multiyear average of the sea level pressure isobars and geostrophic winds derived from a daily average of the European Centre for Medium-Range Weather Forecasts (ECMWF) interim analysis fields. These fields are available on a 1.125 degree latitude-longitude grid, that we regridded to 100 km and used throughout the paper. For the Weddell, a low-pressure system produces offshore winds at the northeast coast, and easterly winds in the south. For the Ross, a low-pressure system to the east produces strong southerly winds off the western Ross Ice Shelf. Figures 1c and 1d show the locations of the straight-line flux gates, where the Ross gate is identical to that used by *Martin et al.* [2007]. Figures 1c and 1d show for the above time period, the multiyear means of the daily ice motion vectors (IMV) derived from the 89-GHz AMSR-E channels [*Kwok*, 2005]. Figure 1c and 1d show that the ice drift closely follows the geostrophic winds, and that in the Ross, the strongest ice export occurs north of the Ross Ice Shelf, while in the Weddell, it occurs off the east coast. For 2003–2008, Table 1 lists the net area export across the flux gate, and shows that on average, the Ross export is approximately twice that of the Weddell.

3. Ice Production in the Ross and Weddell Sea Polynyas

[5] Our ice production calculation uses the brightness temperature ratio of the 12.5-km resolution AMSR-E 36-GHz channels to calculate the polynya ice thicknesses (0–15 cm). *Martin et al.* [2005] derive the algorithm in the Chukchi Sea; *Kwok et al.* [2007, Figure 5] validate the identical algorithm in the Ross Sea. From these daily distributions of ice thicknesses and assuming that the seawater is at its freezing point, the winter heat flux and ice production is calculated from the ECMWF atmospheric temperatures and geostrophic winds, with the error in the annual ice production estimated at about ±30% [*Martin et al.*, 2004, 2005]. For the two seas, Figure 2 shows the cumulative ice production. The Weddell ice production occurs primarily in three regions: around the

[1] School of Oceanography, University of Washington, Seattle, Washington, USA.

[2] Jet Propulsion Laboratory, California Institute of Technology, Pasadena, California, USA.

0094-8276/11/2011GL048668

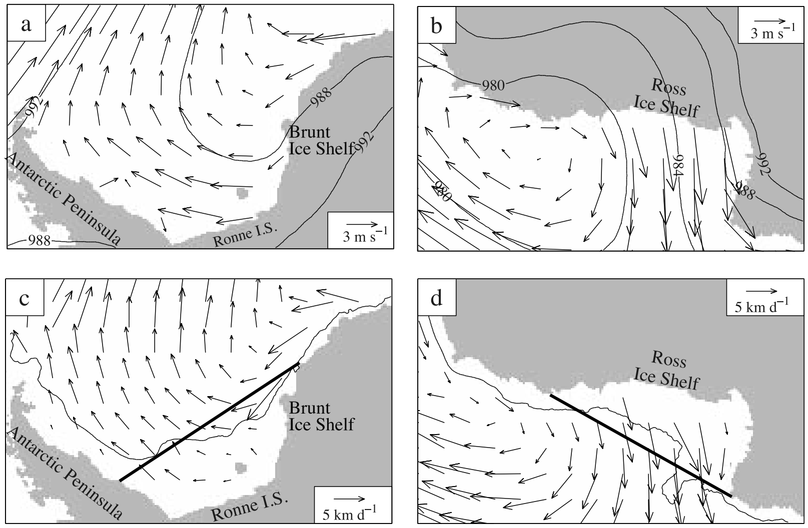

Figure 1. For 2003–2008, the mean isobars of sea level pressure, geostrophic velocities and ice drift velocities for (a) Weddell and (b) Ross; (c) Weddell and (d) Ross ice velocities. In Figures 1c and 1d, the straight black lines are the flux gates; the irregular black lines, the 1,000 m depth contours. See inserts for velocity magnitudes and text for further description.

Brunt Ice Shelf, which we call the Eastern Weddell Polynya (EWP), at the Ronne Ice Shelf and around stationary iceberg A23; the Ross production occurs in the Ross Shelf Polynya (RSP) and the Terra Nova Bay (TNB) and McMurdo Sound (MCM) polynyas. The boxes outline the areas used to calculate the ice production, where land mask is derived from Moderate Resolution Imaging Spectroradiometer (MODIS) imagery. To keep our calculations over the shelves, the northern edge of the EWP and RSP boxes lie along the 1,000-m contour.

[6] For each polynya, the ice production is averaged over 1 April – 30 October 2003–2008, with the two exceptions for the EWP: in 2005, we begin ice production on 9 April; in 2006, on 13 April. This is because the AMSR-E imagery suggests that until these dates, above-freezing open water still exists in the northern EWP box. Figure 2 shows that the EWP and Ronne have maximum production rates of about 15 m y^{-1}. For the Ross, the majority of the production occurs in the RSP, which has a maximum growth rate of about 27.5 m yr^{-1}, where the TNB rates are comparable, while the MCM rates are smaller. For the different polynyas, Table 2 shows the AMSR-E ice production. From Table 2,

Table 1. The Net Areal Ice Export in the Ross and Weddell Seas in Units of 10^5 km^2 Through Their Respective 1,000-m Flux Gates Calculated From AMSR-E[a]

Year	Ross Sea Net Areal Export	Weddell Sea Net Areal Export
2003	8.6	4.9
2004	11.0	3.0
2005	10.0	6.4
2006	7.7	6.4
2007	8.6	5.2
2008	10.3	5.5
Average	9.3	5.2

[a]From *Kwok* [2005, p. 3766], the standard deviation is about 3%, and net refers to the difference between inflow and outflow.

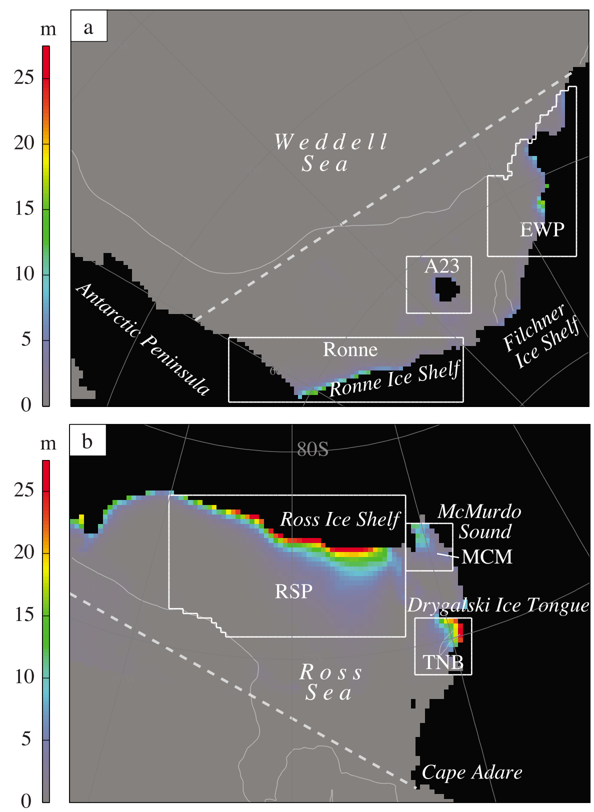

Figure 2. The polynya locations and flux gates (dashed lines) and 1,000-m depth contour for the (a) Weddell and (b) Ross Seas. The colors show the mean annual ice growth per unit pixel derived from AMSR-E for 2003–2008. See text for further description.

Table 2. Annual AMSR-E Weddell and Ross Ice Production by Region in Units of km^3, With Errors of Approximately ±30%[a]

Year	EWP (km^3)	Ronne (km^3)	A23 (km^3)	Weddell Total (km^3)	RSP (km^3)	TNB (km^3)	MCM (km^3)	Ross Total (km^3)
2003	132	100	23	255	589	70	73	731
2004	89	54	18	161	602	90	32	724
2005	138	79	35	252	649	111	11	772
2006	127	177	19	323	510	66	40	615
2007	63	70	21	154	730	99	80	908
2008	125	115	63	303	529	91	47	667
Average	112	99	30	241	602	88	47	737

[a]For the averages, the standard error of the mean is ±12%. See text for further description.

the average Ross production is 740 ± 90 km^3, and the average Weddell production is 240 ± 30 km^3, so that the Ross production is about three times the Weddell. Since 82% of the mean Ross ice production occurs in the RSP, the average RSP production of 600 km^3 exceeds the Weddell total by a factor of 2.5.

[7] For comparison of Table 1 with previous winter studies, *Martin et al.* [2007] find for 1992–2002, a mean RSP production of about 500 km^3. For 1992–2001, *Tamura et al.* [2008] find for the RSP, a production of 390 ± 60 km^3 and for the Ronne, 84.6 ± 25 km^3 consistent with Table 2. They do not report values for the eastern Weddell. For the Weddell, *Renfrew et al.* [2002] find a mean Ronne production of 110 km^3, also consistent with Table 2. For 1992–1994, *Markus et al.* [1998] find that the Ronne average production is 87 km^3 and the EWP is 70 km^3, where these values are slightly smaller than ours. Their larger production in the Ronne is the reverse of our case, where the EWP provides 50% of the total production and the Ronne provides 40%.

[8] Calculation of the exported ice volume depends on the ice thickness. For the Ross, *Martin et al.* [2007] use an average of the ice thicknesses measured by *Jeffries and Adolphs* [1997] from shipboard inside the flux gate in the western Ross Sea during May–June 1995, where they found an average thickness of 0.6 ± 0.3 m. For the southern Weddell, we use ICESat-retrieved ice thicknesses from *Yi et al.* [2011, Figure 4] for the comparable period of May–June, 2004–2006. Their data suggest that neglecting the thick multiyear ice, the ice inside the flux gate has a thickness of 0.75 ± 0.25 m. For comparison, Table 3 lists an ice thickness calculated from division of the ice production in Table 2 by the net areal export in Table 1, where the last column gives the thicknesses from *Jeffries and Adolphs* [1997] and *Yi et al.* [2011]. From Table 3, the multiyear average Ross thickness is twice that of the Weddell, and approximately equal to the observed. This implies that for the Ross and the 1,000-m flux gate, the ice production approximately equals the net volume flux; while for the Weddell, the ice production provides about 60% of the net flux, so that additional ice production must occur in offshore leads.

[9] For the Weddell and for 1992–1998, from passive microwave estimates of the sea ice area, *Renfrew et al.* [2002] assume a 0.5 m ice thickness and find an average ice volume of 1,800 km^3, so that in their case, the Ronne polynya accounts for 4–9% of the total Weddell sea ice. Similarly, for 1992–1994 and an assumed 1-m average thickness, *Markus et al.* [1998] show that their Weddell polynyas produce between 2.5–5% of the total sea ice volume. For our Weddell calculations and an ice thickness of 0.75 ± 0.25 m, the polynyas provide about 5–10% of the total ice volume consistent with earlier estimates; for the Ross, they provide 20–50%. The cause of this difference is the large ice production in the Ross Sea relative to the Weddell.

[10] Even though the SSM/I 37-GHz pixel size is 25 km or twice that of AMSR-E, we use this data to extend the polynya time series to 1992–2008, following *Martin et al.* [2007] and *Comiso et al.* [2011]. Figures 3a–3c show the results for the EWP, the Ronne and their total, where because of its small size, we neglect A23. Figure 3d shows the total Ross ice production, where for 2000–2002, we use the same iceberg masks as *Martin et al.* [2007]. The Ronne polynya has a decreasing trend of −7.9 km^3 y^{-1} that is significant at the 95% confidence level, and the total Ross production has a trend of +20.9 km^3 y^{-1} significant at 99%. Neither the EWP trend of +3.0 km^3 y^{-1} nor the trend of the Ronne and EWP sum of −4.8 km^3 y^{-1} are significant at the 95% level. As Figure 3d shows, while the lower resolution SSM/I production values are slightly smaller than the AMSR-E values, the two estimates are well correlated.

4. Summary and Conclusions

[11] Using flux gates that parallel the 1000-m isobaths and calculating the polynya productivity, we find that the Ross and Weddell Seas have different behaviors. For the Ross, the net ice export approximately equals the polynya ice production; and the ice production is about three times that in the Weddell, and the ice export is about two times, so that using the observed ice thicknesses, the Weddell polynyas provide about 60% of the observed flux. Also, the Ross

Table 3. Ice Thickness (m) Needed to Balance the Ice Production and Net Export for the Winter Period April–November[a]

Year/Thickness (m)	2003	2004	2005	2006	2007	2008	Average	Observed
Weddell	0.5 ± 0.2	0.5 ± 0.2	0.4 ± 0.1	0.5 ± 0.2	0.3 ± 0.1	0.5 ± 0.2	0.4 ± 0.05	0.75 ± 0.25
Ross	0.9 ± 0.3	0.7 ± 0.2	0.8 ± 0.3	0.8 ± 0.3	1.1 ± 0.3	0.6 ± 0.2	0.8 ± 0.1	0.6 ± 0.3

[a]For the average, the uncertainty is the standard error of the mean. The last column gives the *Yi et al.* [2011] satellite thicknesses for the Weddell and the *Jeffries and Adolphs* [1997] observed thicknesses for the Ross. See text for further description.

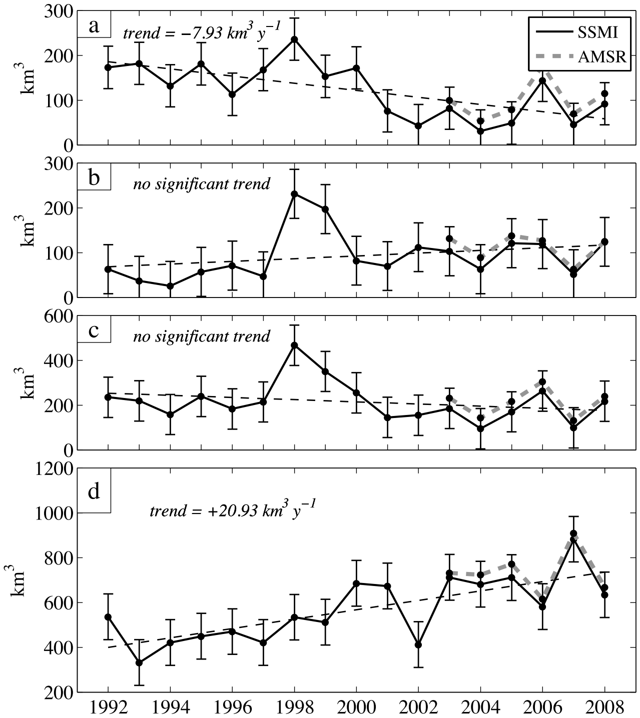

Figure 3. Annual SSM/I ice production for (a) Ronne, (b) EWP, (c) their sum, (d) Ross Sea, for 1992–2008 (solid line), and 2003–2008 for AMSR-E (gray dashed line). The thin dashed lines show the trends; the vertical scales of 3c and 3d are respectively two and four times that of 3a and 3b. The error bars are ±one standard deviation of the residuals, and equal 47.2, 54.5, 89.7 and 101.8 km^3 respectively. See text for further description.

production provides 20–50% of maximum sea ice volume; the Weddell provides 5–10%. In contrast to earlier work, which shows that the Ronne polynya is dominant, we find for the Weddell that the Ronne production is about 40% of the total polynya ice production, with 50% occurring in the Eastern Weddell Polynya. Finally, for 1992–2008, the Ross production increases at a rate of about 21 km^3 per year, while in the Weddell, the Ronne polynya has a significant decreasing trend of about −8 km^3 per year, and the sum of the Ronne and the EWP has no significant trend.

[12] **Acknowledgments.** SM and RD acknowledge the NASA support under contract NNG04GM69G. RK performed this work at the Jet Propulsion Laboratory under contract with NASA. We thank the National Snow Ice Center (NSIDC) for provision of the AMSR-E and SSM/I data.

[13] The Editor wishes to thank Ian Renfrew and two anonymous reviewers for their assistance evaluating this paper.

References

Comiso, J. C., and A. L. Gordon (1998), Interannual variability in summer sea ice minimum, coastal polynyas and bottom water formation in the Weddell Sea, in *Antarctic Sea Ice: Physical Processes, Interaction, and Variability*, *Antarct. Res. Ser.*, vol. 74, edited by M. O. Jeffries, pp. 293–315, AGU, Washington, D. C.

Comiso, J. C., R. Kwok, S. Martin, and A. L. Gordon (2011), Variability and trends in sea ice extent and ice production in the Ross Sea, *J. Geophys. Res.*, *116*, C04021, doi:10.1029/2010JC006391.

Jacobs, S. S. (2004), Bottom water production and its links with the thermohaline circulation, *Antarct. Sci.*, *16*, 427–437, doi:10.1017/S095410200400224X.

Jeffries, M. O., and U. Adolphs (1997), Early winter ice and snow thickness distribution, ice structure and development of the western Ross Sea pack ice between the ice edge and the Ross Ice Shelf, *Antarct. Sci.*, *9*, 188–200, doi:10.1017/S0954102097000242.

Kwok, R. (2005), Ross Sea ice motion, area flux, and deformation, *J. Clim.*, *18*, 3759–3776, doi:10.1175/JCLI3507.1.

Kwok, R., J. C. Comiso, S. Martin, and R. Drucker (2007), Ross Sea polynyas: Response of ice concentration retrievals to large areas of thin ice, *J. Geophys. Res.*, *112*, C12012, doi:10.1029/2006JC003967.

Markus, T., C. Kottmeier, and E. Fahrbach (1998), Ice formation in coastal polynyas in the Weddell Sea and their impact on oceanic salinity, in *Antarctic Sea Ice: Physical Processes, Interaction, and Variability*, *Antarct. Res. Ser.*, vol. 74, edited by M. O. Jeffries, pp. 293–315, AGU, Washington, D. C.

Martin, S., R. Drucker, R. Kwok, and B. Holt (2004), Estimation of the thin ice thickness and heat flux for the Chukchi Sea Alaskan coast polynya from Special Sensor Microwave/Imager data, 1990–2001, *J. Geophys. Res.*, *109*, C10012, doi:10.1029/2004JC002428.

Martin, S., R. Drucker, R. Kwok, and B. Holt (2005), Improvements in the estimates of ice thickness and production in the Chukchi Sea polynyas derived from AMSR-E, *Geophys. Res. Lett.*, *32*, L05505, doi:10.1029/2004GL022013.

Martin, S., R. S. Drucker, and R. Kwok (2007), The areas and ice production of the western and central Ross Sea polynyas, 1992–2002, and their relation to the B-15 and C-19 iceberg events of 2000 and 2002, *J. Mar. Syst.*, *68*, 201–214, doi:10.1016/j.jmarsys.2006.11.008.

Renfrew, I. A., J. C. King, and T. Markus (2002), Coastal polynyas in the southern Weddell Sea: Variability of the surface energy budget, *J. Geophys. Res.*, *107*(C6), 3063, doi:10.1029/2000JC000720.

Tamura, T., K. I. Ohshima, and S. Nihashi (2008), Mapping of sea ice production for Antarctic coastal polynyas, *Geophys. Res. Lett.*, *35*, L07606, doi:10.1029/2007GL032903.

Yi, D., H. J. Zwally, and J. W. Robbins (2011), ICESat observations of seasonal and interannual variations of sea-ice freeboard and estimated thickness in the Weddell Sea, Antarctica (2003–2009), *Ann. Glaciol.*, *52*(57), 43–51, doi:10.3189/172756411795931480.

R. Drucker and S. Martin, School of Oceanography, University of Washington, Box 357940, Seattle, WA 98195-7940, USA. (robert@ocean.washington.edu; seelye@u.washington.edu)

R. Kwok, Jet Propulsion Laboratory, California Institute of Technology, 4800 Oak Grove Dr., Pasadena, CA 91109, USA. (ronald.kwok@jpl.nasa.gov)